

This is the peer reviewed version of the following article:

Mitigation of Electrical/Ionic Interference in Iontronic Neurostimulation/Neurosensing Platforms: A Simulation Study / Nicolini, Jacopo; Leva, Federico; Palestri, Pierpaolo; Selmi, Luca. - (2023), pp. N/A-N/A. (Intervento presentato al convegno 2023 IEEE SENSORS, SENSORS 2023 tenutosi a Vienna nel 29/10/2023-1/11/2023) [10.1109/SENSORS56945.2023.10324927].

Institute of Electrical and Electronics Engineers Inc.

Terms of use:

The terms and conditions for the reuse of this version of the manuscript are specified in the publishing policy. For all terms of use and more information see the publisher's website.

28/04/2025 02:14

(Article begins on next page)

Mitigation of electrical/ionic interference in iontronic neurostimulation/neurosensing platforms: a simulation study

Jacopo Nicolini^{1*}, Federico Leva¹, Pierpaolo Palestri², Luca Selmi¹

¹Department of Engineering “Enzo Ferrari”, University of Modena and Reggio Emilia, Modena, Italy

²Polytechnic Department of Engineering and Architecture, University of Udine, Italy

*E-mail: jacopo.nicolini@unimore.it

Abstract—In the context of *in-vitro* neural interfaces for neurostimulation via extracellular calcium modulation, we investigated by finite element numerical simulations the electrical cross-talk between a polymeric ionic actuator for calcium release and a microelectrode for neural recording. Several device designs have been explored to mitigate the cross-talk. A separation wall between the ionic emitter and the sensing electrode has been found to remarkably improve the ratio between the sensed action potentials and the disturb induced by ionic actuation.

Index Terms—neuromodulation, ionic actuation, calcium release, microelectrodes, cross-talk, conductive polymers

I. INTRODUCTION

Conductive polymer/polyelectrolyte blends (CP/PE) are a topic of intense research for bioelectronics and neurobiology applications [1]–[3], notably for the development of transparent electrodes [4] and organic-electronic ion pumps [5].

Integrating this new technology on the same chip with existing microelectrode arrays (MEAs) for extracellular sensing and stimulation [6]–[8] would open new pathways in experimental neuroscience towards coordinated *in vitro* ionic neurostimulation and electrical neurosensing [9]–[12]. However, the typical magnitude of the neuronal extracellular signals (\approx hundreds of microvolts [8]) is much smaller than that of intracellular ones recorded by patch clamps [13] [14]. Extracellular signals are thus vulnerable to electrical disturbs (e.g., from neurons not directly facing the electrode, chemical reactions and local concentration gradients at the electrode surface, capacitive coupling of the actuation signals, etc.) and demand a careful system design, attentive to the coupling among the stimulation and sensing electrodes.

In this work, we investigate by means of finite elements multiphysics simulations a template prototypical neurostimulation and sensing system formed by a planar sensing microelectrode, an electrode coated with a calcium-selective conductive polymer (CP) for ion release, and a neuron. As a relevant case study, we focus on extracellular calcium ion gradients [15], which have been shown to switch the neuron firing mode from bursting (at low calcium levels typical of epileptic seizures) to tonic interspike intervals (ISI) at the physiological calcium concentration (\approx 2 mM) [16]. A wide range of geometrical

configurations is explored in search for optimal designs to mitigate the cross-talk.

II. METHODOLOGY

We used COMSOL[®] [17] as a finite element method (FEM) simulation environment with multiscale and multiphysics capabilities. This choice allows us to easily scale the model in terms of geometrical dimensions and to quickly add descriptions of new physics and electrochemical phenomena. The equation sets in the different physical domains and related boundaries are listed below and summarized in Figure 1.

The intra- and extra-cellular electrolytes model is based on the Poisson-Nernst-Planck (PNP) equations that govern the electrostatics and diffusion of H, OH, K, Cl, Na and Ca ions.

The neuronal membrane is described by an augmented Hodgkin-Huxley (HH) model, including calcium ion channels and calcium-controlled K⁺ ion channels [18] with larger area density in the vicinity of the sensing electrode [19].

The polymer coating is poly (3,4-ethylenedioxythiophene) polystyrene sulfonate (PEDOT:PSS), which is assumed calcium-selective. It is described as a two-phase system, and reproduces the volumetric capacitance effect observed in [20].

The microelectrode sensor and its surface charge induced by site binding reactions are described by a Markov chain dynamic model as in [21] and [22].

We successfully validated the implementation of all these models vs the experiments reported in the referenced papers. The system dimensions are defined in Figure 2 and their values are reported in the caption. Parameter sweeps are specified in the legends of the figures.

III. RESULTS

The conductive polymer ion emitter is stimulated at the bottom contact with a 18 ms, $s=10$ mV/ms voltage ramp (unless stated otherwise) which are realistic values to raise the extracellular calcium concentration from an abnormal low level of 0.5 mM (typical of epileptic episodes) to the physiological 2 mM value [23]. The voltage ramp triggers the release of calcium ions stored in the polymer. The ramp couples to the sensing electrode potential (ϕ_{sens}) via the high dielectric permittivity electrolyte, thus interfering with the recording of extracellular action potentials (EAPs). Figure 3 shows that

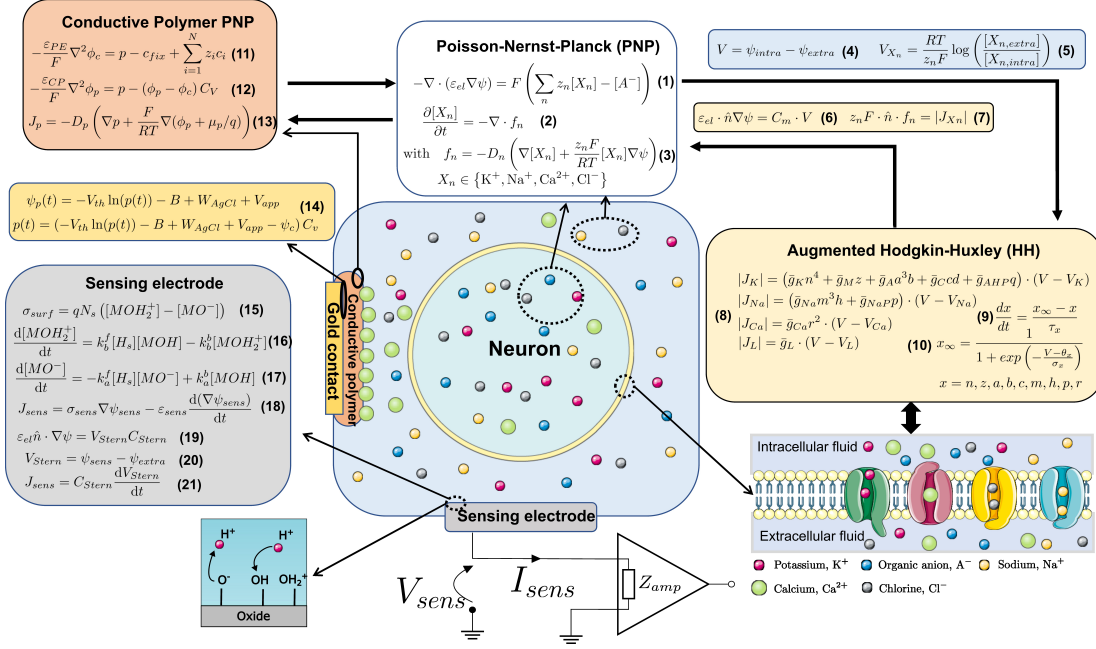


Fig. 1: Summary of the adopted multiphysics model equations, including the two-phase model of the conductive polymer, the site binding charge model on the electrode surface, the Poisson-Nernst-Planck (PNP) model for the electrolyte and the augmented Hodgkin-Huxley (HH) model for the neuronal membrane. The central part of the figure is a conceptual sketch of the system connecting the domains and their boundaries to the corresponding model equations.

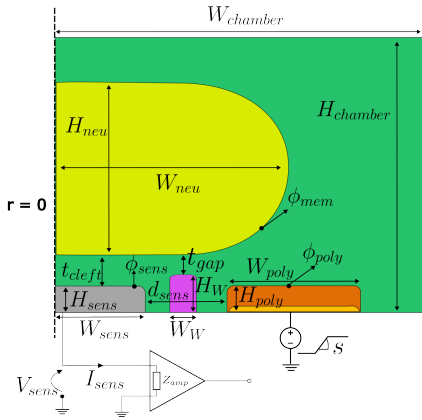


Fig. 2: Sketch of the half cross section and definition of dimensions for the template neurostimulation/neurosensing system under study. Cylindrical coordinates around the $r=0$ axis are used. Dimensions are: $H_{chamber}=40 \mu m$, $W_{chamber}=40 \mu m$, $H_{neu}=7 \mu m$, $W_{neu}=8.5 \mu m$, $W_W=1 \mu m$, $H_{sens}=0.6 \mu m$, $W_{sens}=3 \mu m$, $H_{poly}=0.6 \mu m$, $W_{poly}=3.5 \mu m$, $t_{left}=50 nm$.

without neuron, the few hundred millivolt actuation potential generates a few hundred microvolt ϕ_{sens} disturb, regardless of the presence or not of dynamic site binding phenomena which appear too slow to appreciably affect the waveforms.

Figure 4a indicates that the magnitude of the disturb increases with the slope s and magnitude of the actuation signal

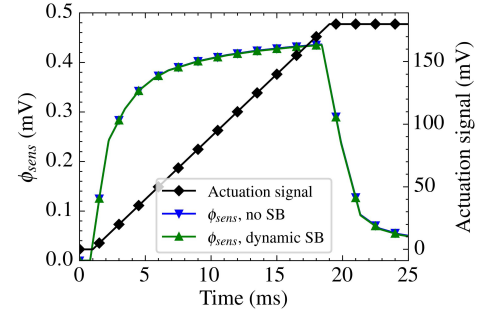


Fig. 3: Actuation potential ramp and sensed potential waveforms during a typical calcium ion release event without neuron, and with or without dynamic site binding reactions (parameters from [22]).

(at constant duration of the ramp, 18 ms). This is consistent with experiments in [20] where the polymer undergoes cyclic voltammetry at different scan rates.

In order to mitigate the electrical crosstalk during ionic actuation, we firstly increased the distance between the actuator and the sensor, d_{sens} , Figure 4b, however achieving only a modest reduction of the interference, with the additional downside of higher calcium diffusion times to the neuron.

An alternative solution is to insert a conductive, grounded, ring-shaped wall between the sensor and the polymer or, alternatively, an insulating one ($\varepsilon_r = 3.9$). By interrupting the field/current paths between electrodes, both wall implementations reduce the electrical crosstalk for increasing wall

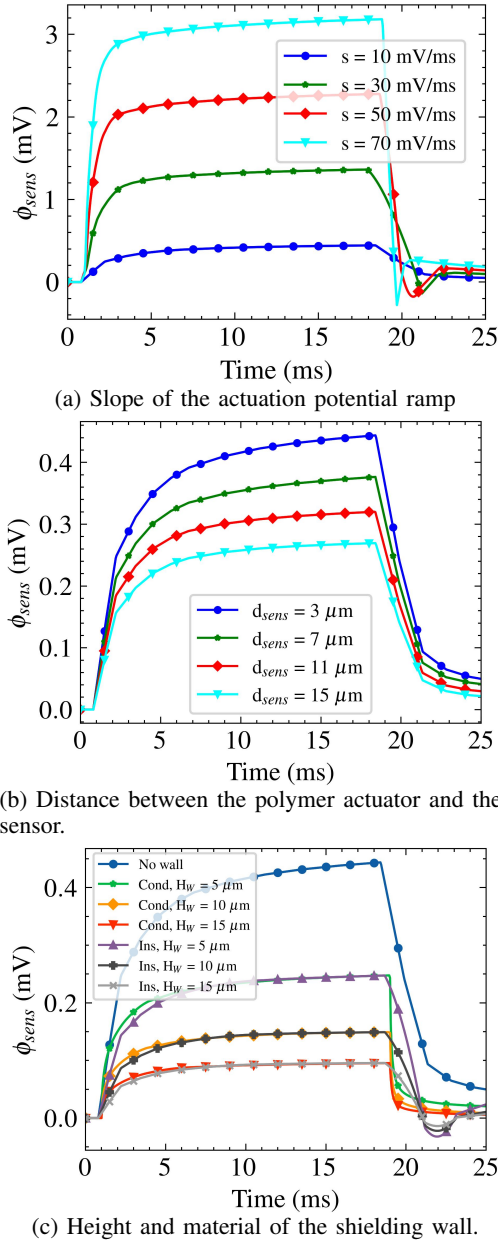


Fig. 4: Potential waveforms on the sensing electrode for different simulation parameters in the absence of the neuron.

height by about the same amount, as shown in Figure 4c. The conductive wall yields a faster decay of the interference compared to the insulating one, which is beneficial to contain the blind recording period.

Figure 5 (top graph) reports the sensing electrode waveforms in the presence of an active or inactive neuron located at $t_{cleft}=50$ nm and without the shielding wall. We see that the presence of an inactive neuron (i.e., with blocked ionic channels) increases the level of interference compared to the case without neuron. Indeed, when the neuron approaches the sensing electrode and the polymer the spreading resistance towards the reference electrode increases. Therefore, the sensing electrode becomes more disconnected from the RE, thus

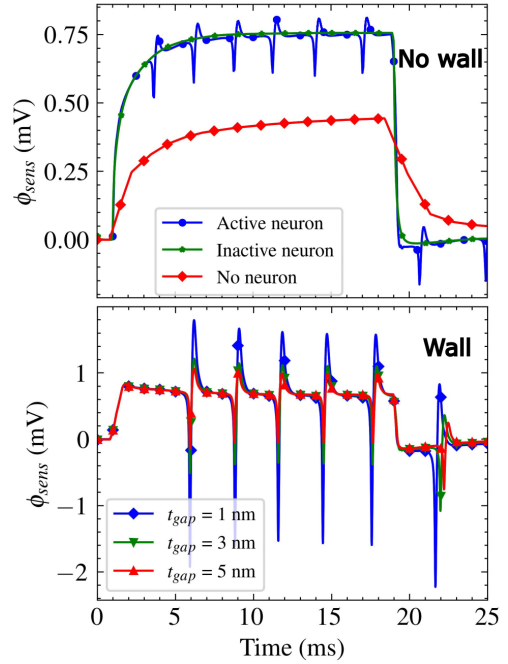


Fig. 5: Sensing electrode potential during ionic actuation with neuron and without (top) or with (bottom) the wall. The APs superimpose to the actuator signal. The APs are amplified as t_{gap} is reduced.

being more prone to capture the disturbance from the actuator. When the neuron is active, we still have a large interfering signal, but superimposed APs are visible with an approximate signal-to-interference ratio $SIR = 20 \log_{10} \frac{200 \mu V}{700 \mu V} \approx -11$ dB. Figure 5 (bottom graph) shows that, upon insertion of an insulating wall, biphasic waveforms with increasing amplitude are captured by the electrode as t_{gap} decreases, in agreement with the trend in [24] when the sealing resistance increases. The insulating wall remarkably improves the amplitude of the sensed action potential, leading to an enhanced $SIR \approx 4.3$ dB.

IV. CONCLUSIONS

The exploration of a new neuromodulation-neurosensing platform by multiphysics, multiscale simulation highlighted the existence of a large cross-talk between the ionic actuator and the sensing microelectrode. Indeed, the polymer actuation signal generates an interfering waveform difficult to mitigate when realizing ion delivery towards an overlaying neuron. Increasing the distance between the stimulation and sensing electrodes yields modest SIR improvements at the expense of a trade-off between the speed of ion diffusion to the neuron and the sensor immunity to interference. The fabrication of an insulating separation wall surrounding the sensor effectively amplifies the useful signal and remarkably improves the SIR. *These results shed new light on the microelectrode transduction mechanisms in the presence of ionic actuation and pave the way to efficient signal filtering and system design.*

Acknowledgments: We would like to thank Claudio Verardo (Scuola S.Anna, Pisa) for useful discussions and advice.

REFERENCES

- [1] K. Tybrandt, R. Forchheimer, and M. Berggren, "Logic gates based on ion transistors," *Nature communications*, vol. 3, no. 1, p. 871, 2012.
- [2] D. T. Simon, S. Kurup, K. C. Larsson, R. Hori, K. Tybrandt, M. Gojny, E. W. Jager, M. Berggren, B. Canlon, and A. Richter-Dahlfors, "Organic electronics for precise delivery of neurotransmitters to modulate mammalian sensory function," *Nature materials*, vol. 8, no. 9, pp. 742–746, 2009.
- [3] E. Frantz, J. Huang, D. Han, and A. J. Steckl, "The effect of nutrient broth media on pedot: Pss gated oects for whole-cell bacteria detection," *Biosensors and Bioelectronics: X*, vol. 12, p. 100268, 2022.
- [4] Y. Wang, C. Zhu, R. Pfattner, H. Yan, L. Jin, S. Chen, F. Molina-Lopez, F. Lissel, J. Liu, N. I. Rabiah, *et al.*, "A highly stretchable, transparent, and conductive polymer," *Science advances*, vol. 3, no. 3, p. e1602076, 2017.
- [5] J. Isaksson, P. Kjäll, D. Nilsson, N. Robinson, M. Berggren, and A. Richter-Dahlfors, "Electronic control of ca2+ signalling in neuronal cells using an organic electronic ion pump," *Nature materials*, vol. 6, no. 9, pp. 673–679, 2007.
- [6] S. Martinoia, P. Massobrio, M. Bove, and G. Massobrio, "Cultured neurons coupled to microelectrode arrays: circuit models, simulations and experimental data," *IEEE Transaction on Biomedical Engineering*, vol. 51, no. 5, pp. 859–863, 2004. 10.1109/TBME.2004.826607.
- [7] G. Massobrio, S. Martinoia, and P. Massobrio, "Equivalent circuit of the neuro-electronic junction for signal recordings from planar and engulfed micro-nano-electrodes," *IEEE Transactions on Biomedical Circuits and Systems*, vol. 12, no. 1, pp. 3–12, 2018. 10.1109/TBCAS.2017.2749451.
- [8] M. E. Spira and A. Hai, "Multi-electrode array technologies for neuroscience and cardiology," *Nature nanotechnology*, vol. 8, no. 2, pp. 83–94, 2013. 10.1038/nnano.2012.265.
- [9] A. Jonsson, S. Inal, I. Uguz, A. J. Williamson, L. Kergoat, J. Rivnay, D. Khodagholy, M. Berggren, C. Bernard, G. G. Malliaras, *et al.*, "Bioelectronic neural pixel: Chemical stimulation and electrical sensing at the same site," *Proceedings of the National Academy of Sciences*, vol. 113, no. 34, pp. 9440–9445, 2016.
- [10] Y. Liang, A. Offenhäusser, S. Ingebrandt, and D. Mayer, "Pedot: Pss-based bioelectronic devices for recording and modulation of electrophysiological and biochemical cell signals," *Advanced Healthcare Materials*, vol. 10, no. 11, p. 2100061, 2021.
- [11] F. Hu, Y. Xue, J. Xu, and B. Lu, "Pedot-based conducting polymer actuators," *Frontiers in Robotics and AI*, vol. 6, p. 114, 2019.
- [12] A. S. Pranti, A. Schander, A. Bödecker, and W. Lang, "Pedot: Pss coating on gold microelectrodes with excellent stability and high charge injection capacity for chronic neural interfaces," *Sensors and Actuators B: Chemical*, vol. 275, pp. 382–393, 2018.
- [13] J. Abbott, T. Ye, K. Krenek, R. S. Gertner, W. Wu, H. S. Jung, D. Ham, and H. Park, "Extracellular recording of direct synaptic signals with a cmos-nanoelectrode array," *Lab Chip*, vol. 20, pp. 3239–3248, 2020. 10.1039/D0LC000553C.
- [14] J. Abbott, T. Ye, K. Krenek, L. Qin, Y. Kim, W. Wu, R. S. Gertner, H. Park, and D. Ham, "The design of a cmos nanoelectrode array with 4096 current-clamp/voltage-clamp amplifiers for intracellular recording/stimulation of mammalian neurons," *IEEE Journal of Solid-State Circuits*, vol. 55, no. 9, pp. 2567–2582, 2020. 10.1109/JSSC.2020.3005816.
- [15] R. Rasmussen, J. O'Donnell, F. Ding, and M. Nedergaard, "Interstitial ions: A key regulator of state-dependent neural activity?," *Progress in neurobiology*, vol. 193, p. 101802, 2020.
- [16] C. Yue, S. Remy, H. Su, H. Beck, and Y. Yaari, "Proximal persistent na+ channels drive spike afterdepolarizations and associated bursting in adult ca1 pyramidal cells," *Journal of Neuroscience*, vol. 25, no. 42, pp. 9704–9720, 2005.
- [17] Comsol, Inc., Comsol Multiphysics v. 6.0.
- [18] D. Golomb, C. Yue, and Y. Yaari, "Contribution of persistent na+ current and m-type k+ current to somatic bursting in ca1 pyramidal cells: combined experimental and modeling study," *Journal of neurophysiology*, vol. 96, no. 4, pp. 1912–1926, 2006.
- [19] P. Massobrio, G. Massobrio, and S. Martinoia, "Interfacing cultured neurons to microtransducers arrays: A review of the neuro-electronic junction models," *Frontiers in Neuroscience*, vol. 10, no. JUN, 2016. 10.3389/fnins.2016.00282.
- [20] K. Tybrandt, I. V. Zozoulenko, and M. Berggren, "Chemical potential–electric double layer coupling in conjugated polymer–polyelectrolyte blends," *Science advances*, vol. 3, no. 12, p. eaao3659, 2017.
- [21] L. J. Mele, P. Palestri, and L. Selmi, "A model of the interface charge and chemical noise due to surface reactions in ion sensitive fet," in *2019 International Conference on Simulation of Semiconductor Processes and Devices (SISPAD)*, pp. 1–4, IEEE, 2019.
- [22] F. Bellando, L. J. Mele, P. Palestri, J. Zhang, A. M. Ionescu, and L. Selmi, "Sensitivity, noise and resolution in a beol-modified foundry-made isfet with miniaturized reference electrode for wearable point-of-care applications," *Sensors*, vol. 21, no. 5, p. 1779, 2021.
- [23] E. R. Kandel, J. D. Koester, S. H. Mack, and S. A. Siegelbaum, *Principles of neural science, sixth edition*. McGraw-Hill Education/Medical, 6 ed., apr 2021.
- [24] P. Fromherz, A. Offenhäusser, T. Vetter, and J. Weis, "A neuron-silicon junction: A retzius cell of the leech on an insulated-gate field-effect transistor," *Science*, vol. 252, pp. 1290–1293, May 1991.